JOURNAL OF VIROLOGY, Dec. 1990, p. 6130–6140
0022-538X/90/126130-11$02.00/0

Vol. 64, No. 12

Substitution of Murine Transthyretin (Prealbumin) Regulatory Sequences into the Moloney Murine Leukemia Virus Long Terminal Repeat Yields Infectious Virus with Altered Biological Properties

GEROLD FEUER† AND HUNG FAN*

Department of Molecular Biology and Biochemistry, University of California, Irvine, California 92717

Received 16 May 1990/Accepted 6 September 1990

The effects of inserting cellular regulatory sequences from the murine transthyretin (TTR) gene into the Moloney murine leukemia virus (M-MuLV) long terminal repeat (LTR) were investigated. Transthyretin is expressed predominantly in the liver and choroid plexus in adult mice, and TTR upstream regulatory elements were previously shown to potentiate transcription in liver-derived cells. The effects of inserting the TTR distal enhancer and/or promoter-proximal sequences into an M-MuLV LTR lacking its enhancers were measured in three ways. (i) Chimeric LTRs were fused to the bacterial chloramphenicol acetyltransferase gene (*cat*) and tested for transient gene expression by transfection into liver-derived cells or NIH 3T3 fibroblasts. (ii) Infectious M-MuLV containing an altered LTR [ΔMo+TTR(PD) MuLV] was generated, and infectivity in culture on hepatocyte lines and NIH 3T3 cells was tested. (iii) Infection of ΔMo+TTR(PD) MuLV in vivo was tested by inoculating NFS/N mice and performing in situ hybridization of whole animal sections. Chimeric LTR-*cat* constructs showed higher levels of *cat* gene expression in liver-derived cell lines than in NIH 3T3 cells, indicating increased LTR activity in these cells. However, in vitro infection did not show significantly higher infectivity in hepatocytes for ΔMo+TTR(PD) M-MuLV than did wild-type M-MuLV. In vivo, ΔMo+TTR(PD) MuLV showed expression in the same tissues as with wild-type M-MuLV-inoculated mice, i.e., lymphoid organs and the intestines and, additionally, two novel sites not seen in wild-type M-MuLV-inoculated animals. Of 10 mice, 8 showed viral expression in the brain and 3 showed expression in the liver. Thus, insertion of TTR elements into the M-MuLV LTR altered LTR activity both in vitro and in vivo.

Retroviruses provide a convenient model system for studying eucaryotic gene regulation. The long terminal repeat (LTR) of Moloney murine leukemia virus (M-MuLV) and the U3 region, in particular, contain sequences important for regulation of viral gene expression and replication (48). In addition to containing characteristic eucaryotic promoter motifs (TATAA and CAAT), the U3 region also contains transcriptional enhancer sequences (28). The M-MuLV enhancers are essential for LTR transcriptional activity in transient expression assays, and they are primary determinants in the tissue tropism (21, 34) and leukemogenicity of infectious M-MuLV (8, 14, 22, 29, 30).

We previously studied the role of enhancer sequences in gene expression and pathogenesis for M-MuLV. By molecular cloning, substitutions and insertions with heterologous viral enhancers resulted in chimeric LTRs that showed altered transcriptional properties in transient expression assays (11, 13, 18, 36). Infectious M-MuLVs containing these altered LTRs also showed altered biological properties in tissue culture and in inoculated mice (10, 17, 18).

Viral enhancers, such as those of simian virus 40 and polyomavirus, potentiate transcription in a broad spectrum of cell types. This presumably reflects in vivo selection for viruses that efficiently infect the host (19, 50). In contrast, certain cellular genes contain enhancers that are highly specific in driving expression in particular cell types (42, 43, 44, 46, 49, 52). Introduction of cellular enhancer elements into the M-MuLV LTR might result in M-MuLVs that show a restricted or altered range of cell types able to support viral expression.

The mouse transthyretin (TTR) gene is transcribed in adults mainly in the liver and choroid plexus (5, 9) and encodes a polypeptide that serves as a carrier for thyroxine. Previous studies have identified upstream distal enhancer and promoter-proximal sequence elements required for cell-specific transcription (4–6). Cellular proteins with limited tissue distribution which bind sequences in the distal enhancer have been identified, implicating these regions in the cell specificity.

In this report, we describe the generation of M-MuLV LTRs carrying the regulatory sequence elements of the TTR gene. The transcriptional activities of these chimeric LTRs were tested in transient assays using hepatocyte cell lines. An infectious M-MuLV driven by the TTR regulatory sequences was also generated. The chimeric M-MuLV had infectivity similar to that of the wild-type M-MuLV for hepatocytes in tissue culture. In contrast, it displayed an expanded pattern of expression in organs of inoculated animals, including the liver and brain.

MATERIALS AND METHODS

Cell lines and viruses. NIH 3T3 cells (47) were grown in monolayers in Dulbecco modified Eagle medium supplemented with 10% calf serum. HepG2 (26) and M-hep (20, 38) cells were grown in Ham F12 medium supplemented with

* Corresponding author.
† Present address: Department of Microbiology and Immunology, University of California at Los Angeles, Los Angeles, CA 90024-1678.

10% fetal bovine serum (Whitaker MA Bioproducts) and 0.2 U of insulin per ml (Eli Lilly & Co.). Virus stocks were obtained by harvesting culture medium from confluently infected cultures and removing cells and cellular debris by centrifugation at 2,000 × *g* for 2 min. Samples of the viral supernatants were stored at −80°C, and each was used only once after thawing. Infectious M-MuLV titers were determined by endpoint dilution or plaque titration on NIH 3T3 cells with the UV-XC syncytial assay (41).

Molecular cloning and DNA transfection. Molecular cloning procedures were done by standard protocols (33). The TTR gene promoter-proximal and enhancer elements have been described previously (5). The TTR promoter-proximal sequences used for all insertions was the 132-bp *Xba*I fragment. The TTR enhancer sequences were also previously subcloned and isolated as an *Xba*I-to-*Hin*dIII fragment. The *Hin*dIII site was end filled with the Klenow fragment of DNA polymerase I and blunt end ligated with kinase-treated *Xba*I linkers.

DNA transfections for all cell lines were performed by the modified calcium phosphate precipitation procedure and have been previously described (3, 13). Cell extracts were prepared 40 h posttransfection, and standardized reactions for bacterial chloramphenicol acetyltransferase (CAT) enzyme activity were performed as previously described (13, 15).

RNase T_2 analysis. Transient expression from the LTR-*cat* fusion constructs was analyzed by RNase T_2 digestion of hybrids between a radioactive antisense RNA probe and cytoplasmic RNA from transfected cells (5, 13, 35). RNA was isolated from cells transfected with the LTR-*cat* constructs by using the Nonidet P-40 lysis method (2). The antisense RNA probe used in this analysis was synthesized by using SP6 RNA polymerase from a plasmid containing the M-MuLV LTR-*cat* gene junction, spanning from the *Xba*I site in the LTR (−150) to an *Eco*RI site in the *cat* gene (+250). Before synthesis of the RNA probe, template DNA was linearized by digestion with *Pst*I, a restriction site located 15 bp 3′ to the LTR-*cat* sequences. This resulted in an antisense probe 445 bp long containing 15 bp of plasmid sequences which allowed us to distinguish between an unhybridized probe that survived RNase T_2 digestion (445-bp fragment) and transcription initiating upstream of −150 bp in the M-MuLV LTR (430-bp fragment). Conditions for hybridization, RNase T_2 digestion, and electrophoresis were as described previously (13).

DNA analysis. Southern blotting procedures were as described previously (1). Briefly, DNA was blotted from agarose gels to nylon membranes as directed by the manufacturer (Dupont, NEN Research Products). Blots were dried and prehybridized in 50% formamide–1 M NaCl–10% dextran sulfate–1% sodium dodecyl sulfate (SDS) at 42°C for 1 to 2 h. Hybridization was overnight at the same temperature with the probe (labeled by the random oligonucleotide primer extension reaction [12]) plus denatured salmon sperm DNA. After washing, blots were subjected to autoradiography on Kodak XAR-5 film with intensifying screens.

Virus-specific RNA hybridization. Virus stocks were harvested by centrifugation (100,000 × *g*, 2 h), pellets were suspended in SDS buffer (10 mM Tris, 0.1 M NaCl, 1 mM EDTA), and SDS was added to a final concentration of 1%. After phenol-chloroform extraction, RNA was suspended in water and serial dilutions were blotted onto a nylon membrane presoaked in 10× SSC (1× SSC is 0.15 M NaCl plus 0.015 M sodium citrate). Blots were dried and hybridized under conditions identical to those used for DNA analysis.

Inoculation of mice and in situ hybridization. NFS/N mice were inoculated (2 days after birth) intraperitoneally with 0.2 ml of an undiluted viral stock. Animals were sacrificed at 3 to 5 weeks of age and prepared for cryomicrotomy as described by Lipkin et al. (32). Briefly, sacrificed animals were shaved, frozen in a dry-ice–ethanol bath and embedded in blocks of O.C.T. embedding medium (Miles Laboratories, Inc.). Cryomicrotome sections (20 to 40 μm thick) were collected directly on nylon membranes and stored on dry ice. For hybridization, sections were immediately fixed by wetting each section five times in paraformaldehyde solution (4% paraformaldehyde, 0.1% glutaraldehyde, 100 mM NaH_2PO_4) and five times in a proteinase K–Nonidet P-40 solution [40 mM 1,4-piperazinebis(ethanesulfonic acid), 10 mM sodium acetate, 1 mM EDTA, 1% Nonidet P-40, 50 μg of proteinase K per ml] and each section was gently washed five times in 3× SSC plus 60 mM sodium PP_i. Sections were allowed to dry overnight and washed three more times in 3× SSC plus 60 mM sodium PP_i. After being dried, sections were prehybridized in 50% formamide–1% SDS–1 M NaCl–10% dextran sulfate for at least 6 h. DNA probes were ^{32}P labeled by nick translation (39), and 0.5 × 10^6 cpm of probe per ml of prehybridization solution was added, along with denatured salmon sperm DNA. Hybridization was done overnight at 42°C. After hybridization, sections were washed twice in 2× SSC at room temperature for 5 min, twice in 2× SSC–0.1% SDS at 65°C for 45 min, and twice in 0.1× SSC for 30 min. Sections were set against Saran Wrap and exposed to film (Kodak XAR-5 or XRP-5) at −70°C.

RESULTS

TTR regulatory sequences and altered LTRs. The regulatory sequences that lie upstream of the murine prealbumin (TTR) gene are illustrated in Fig. 1A. The promoter-proximal element (−70 to −202 bp) and the distal enhancer element (−1.86 to −1.96 kb) were cloned by Costa et al. (5), and these two sequences were used to generate chimeric M-MuLV LTRs.

The altered M-MuLV LTRs used in transient assays were generated by molecular cloning as described previously (36) and are diagrammed in Fig. 1B. Each LTR was fused to the bacterial *cat* gene and assayed for transcriptional activity by transient assays. The ΔMo deletion (−150 to −357) lacked the M-MuLV tandem repeats and has been described previously (31). ΔMo+TTR(D) contained the TTR gene distal enhancer sequences inserted as an *Xba*I fragment into the ΔMo LTR. ΔMo+TTR(P^-D) and ΔMo+TTR(PD) both contained the TTR distal enhancer and promoter-proximal elements inserted as *Xba*I fragments into the ΔMo LTR but differed by the relative orientation of the proximal element. In ΔMo+TTR(P^-D), the TTR promoter-proximal element was in the 3′-to-5′ orientation with respect to the M-MuLV promoter; in ΔMo+TTR(PD), both TTR elements were oriented 5′ to 3′. In both of these constructs, the TTR distal enhancer (D) was positioned closer to the M-MuLV promoter than was the TTR promoter-proximal element (P), opposite to the relative position of these elements in the TTR gene.

CAT activities of TTR–M-MuLV chimeric LTRs. Costa et al. previously presented evidence for liver cell specificity of the TTR distal enhancer when inserted upstream of a heterologous β-globin promoter in a transient assay system (5). In addition, the TTR promoter-proximal element was able to promote transcription in a hepatocyte-specific manner when coupled to a viral enhancer active in multiple cell types.

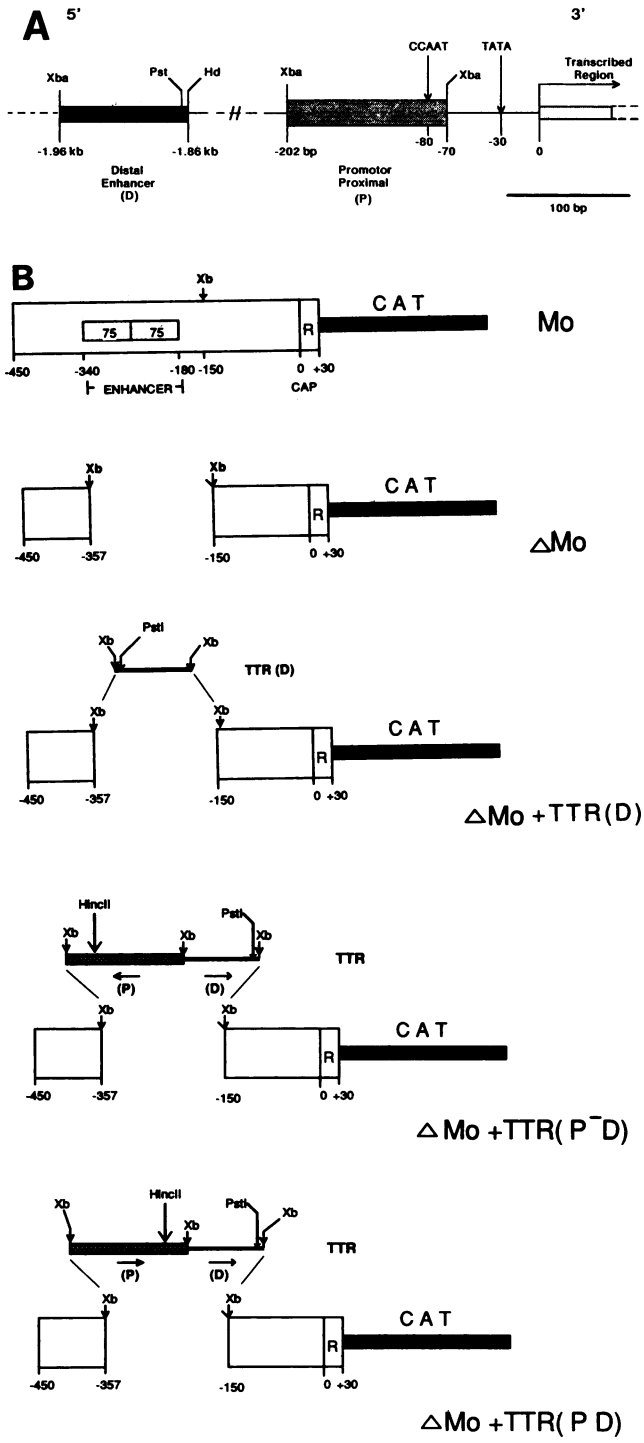

FIG. 1. Chimeric LTRs. (A) Structure of the upstream region of the murine TTR gene. Nucleotide numbering is from the transcriptional start site at 0. The promoter-proximal element encompasses sequences from −70 to −202 bp and contains the CCAAT homology at −80 bp. The distal enhancer sequence is located between −1.86 and −1.96 kb upstream of the TTR transcriptional start site. Originally cloned by Costa et al., these elements were individually cloned and isolated as *Xba*I fragments via *Xba*I linkers. Restriction sites are shown for clarification and were generated during the cloning procedure. (B) LTR-*cat* gene plasmids. Construction of Mo*cat* and ΔMo*cat* has been previously described (7, 36). Constructs contained the entire M-MuLV U3 region and half of the R region attached to the bacterial *cat* gene. The transcriptional start site was at 0, and the standard promoter elements (TATA and CAAT homologies) were located at −30 and −80 bp, respectively. The 75-bp enhancer elements in the U3 region are indicated. ΔMo+TTR(D) represented insertion of the TTR distal enhancer as an *Xba*I fragment into the ΔMo LTR. ΔMo+TTR(PD) and ΔMo+TTR(P⁻D) contained both the TTR promoter-proximal (P) and distal enhancer (D) elements inserted into the ΔMo LTR as *Xba*I fragments. The constructs differed only in the relative orientation of the promoter-proximal element (arrow). In ΔMo+TTR(P⁻D), the promoter-proximal element resides 3′ to 5′ with respect to the M-MuLV LTR, whereas in ΔMo+TTR(PD), both TTR elements lie 5′ to 3′. TTR sequence elements are not drawn to scale.

These results suggested that both the TTR promoter-proximal and enhancer elements contained sequences important for efficient expression in hepatocytes. We wished to test whether these sequences could also confer cell-specific expression to the M-MuLV LTR.

The constructs in Fig. 1B were transfected into M-hep cells, a murine hepatocyte cell line (38), and also into HepG2 (human hepatoma) cells. Cytoplasmic extracts were assayed for CAT activity as a measure of transient expression levels (Fig. 2). For comparison, the same constructs were also transfected into NIH 3T3 fibroblasts. The wild-type M-MuLV LTR and the ΔMo LTR were both inactive in HepG2 cells (Fig. 2A), in agreement with previous results showing that the M-MuLV LTR enhancers are nonfunctional or poorly functional in many human cells (25). Insertion of the TTR distal enhancer element into the ΔMo LTR [ΔMo+TTR(D)] resulted in a small but measurable amount of *cat* expression in HepG2 cells. Constructs containing both of the TTR sequence elements within the ΔMo LTR [ΔMo+TTR(P⁻D)-*cat* and ΔMo+TTR(PD)-*cat*] showed higher levels of CAT activity in HepG2 cells than did ΔMo+TTR(D)-*cat*. Thus, the TTR proximal and distal enhancer elements conferred increased activity to the M-MuLV LTR in the human hepatoma cell line.

In M-hep cells, the wild-type M-MuLV LTR was active (Fig. 2B), presumably because of the high activity of the M-MuLV enhancers in murine cells. Substitutions of the M-MuLV enhancers with the TTR elements also yielded activity, particularly for elements containing both proximal and distal elements [e.g., ΔMo+TTR(P⁻D)]. Comparison with the activities of these LTRs in NIH 3T3 fibroblasts was noteworthy. Relative to the wild-type M-MuLV LTR, ΔMo+TTR(PD) and ΔMo+TTR(D) were more active in M-hep cells than in NIH 3T3 cells, consistent with liver-specific activity. In M-hep cells, ΔMo+TTR(PD)-*cat* and ΔMo+TTR(P⁻D) both showed much higher CAT activities than did ΔMo+TTR(D)-*cat* (Table 1). This suggests that the TTR promoter-proximal and distal enhancer elements function to augment *cat* expression in a synergistic fashion. A summary of the *cat* expression data for each LTR normalized to the M-MuLV LTR in each cell type is presented in Table 1. Note that the apparently high relative levels of expression of the TTR-containing LTRs in HepG2 cells was due to the very low basal activity of the wild-type M-MuLV LTR in these cells.

To ensure that CAT activities of Fig. 2 quantitatively reflected transcription from the M-MuLV cap site, RNase T_2 protection experiments were carried out. Radioactive antisense RNA spanning the M-MuLV transcriptional start site of pMo-*cat* (−150 to +250 bp) was hybridized with total cellular RNA of a transfected cell culture. The hybridization mixture was then digested with RNase T_2, and the protected

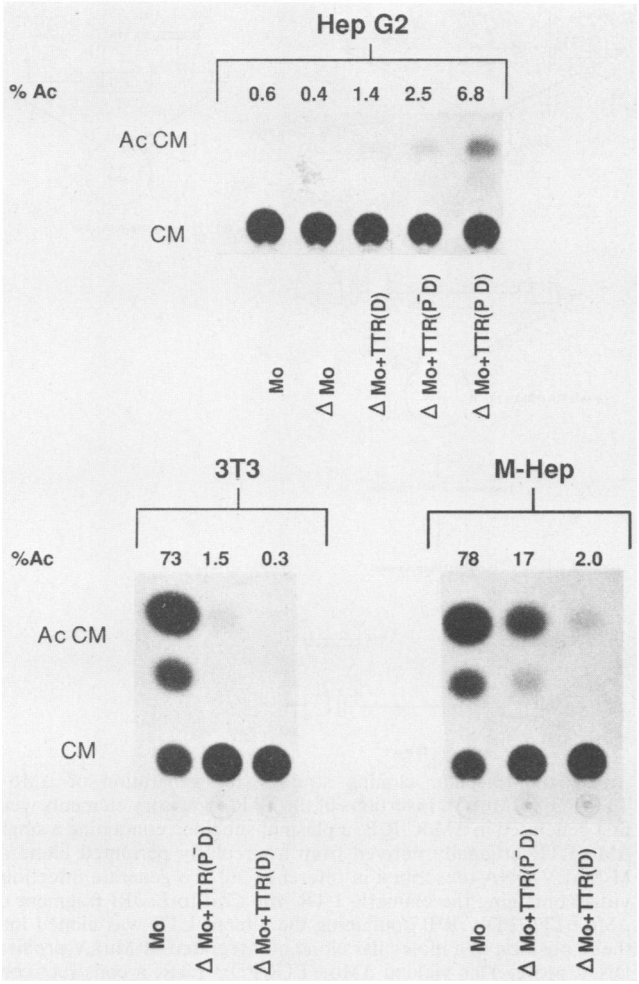

FIG. 2. CAT activities of chimeric LTRs containing TTR regulatory elements. LTR-*cat* expression plasmids were transfected, and CAT enzyme activity was measured as described previously (13). In all cases, 10 μg of plasmid DNA was precipitated in the presence of 10 μg of calf thymus carrier DNA. The amount of cell extract was adjusted for equal A_{280}s, and reactions lasted for identical times. The assays were repeated at least three times with extracts from independent transfections. The amount of acetylation was determined by thin-layer chromatography on silica gel plates and quantified by scintillation counting of excised spots. The locations of the substrate [^{14}C]chloramphenicol (CM) and acetylated forms of chloramphenicol (AcCM) are indicated, as are the levels of acetylation (%Ac).

fragments were analyzed by electrophoresis on a denaturing polyacrylamide gel. The antisense RNA probe was 445 bp long and contained 15 bp of plasmid sequences at the 3′ end. This allowed us to distinguish between the unhybridized probe that survived T_2 digestion and hybrids containing aberrant RNA transcripts initiating upstream of −150 bp in the LTR. The former would yield a 445-bp fragment, while the latter would yield a 430-bp fragment. Transfection of M-hep cells with Mo-CAT, ΔMo+TTR(D)-*cat* and ΔMo+TTR(PD)-*cat* resulted in a 280-bp protected fragment in all cases, signifying correct initiation of transcription from the M-MuLV cap site (Fig. 3). Furthermore, the relative intensities of the protected 280-nucleotide fragments paralleled the amounts of CAT enzyme activity measured. Some aberrant transcription initiating upstream of the *Xba*I site in the M-MuLV LTR (−150 bp) was detected in transfected

TABLE 1. CAT activities of chimeric LTRs[a]

Construct	% Acetylation of chloramphenicol		
	NIH-3T3	M-hep	HepG2[b]
Mo-*cat*	100	100	100
ΔMo	1.9	5.8	58
ΔMo+TTR(D)	1.2	9.6	479
ΔMo+TTR(P⁻D)	1.4	20	1,329
ΔMo+TTR(PD)	4.5	14	3,940

[a] LTR-*cat* expression plasmids were transfected into cells, and extracts were measured for CAT activity as described in Materials and Methods and the legend to Fig. 2. For each experiment, the acetylation value of Mo-*cat* was set at 100% for each cell line and all experimental values were expressed relative to that of Mo-*cat*. The data represent averages from at least three experiments for each LTR and cell line.

[b] Apparent high levels of CAT activity for TTR–M-MuLV LTR constructs in HepG2 cells reflected predominantly the low activity of the wild-type M-MuLV enhancers in HepG2 cells.

cells and resulted in protection of a 430-bp fragment (Fig. 3, arrow). However, the intensities of this band did not correlate with the CAT activities measured, suggesting that these transcripts did not significantly contribute to the CAT activity. In particular, the TTR-containing LTRs did not give higher levels of aberrant transcripts than did the wild-type M-MuLV LTR. Correct initiation of *cat* transcription was also seen in transfected HepG2 and NIH 3T3 cells (data not shown).

Data from these transient assays suggested that insertion of TTR sequence elements resulted in M-MuLV LTRs with higher relative expression in cells of hepatic origin. In addition, insertion of the TTR regulatory sequences allowed the M-MuLV LTR to function more efficiently in human hepatoma cells, a cell type nonpermissive for expression of the wild-type M-MuLV LTR. However, the chimeric TTR-containing LTRs did show activity in nonhepatic cells as well.

Generation of infectious M-MuLV containing ΔMo+TTR(PD) LTRs. Since substitution of the cellular TTR sequence elements conferred new transcriptional properties to the M-MuLV LTR in the transient assays, recovery of infectious M-MuLV containing these chimeric LTRs was attempted. Construction of M-MuLV proviral clones containing the TTR cellular enhancer and proximal promoter elements is illustrated in Fig. 4. Briefly, both TTR sequence elements were inserted into the *Xba*I site of ΔMoC/R/B, an M-MuLV DNA subclone containing an LTR with the ΔMo deletion (36), to give ΔMo+TTR(PD)C/R/B. This clone was then used to generate an M-MuLV provirus plasmid containing a wild-type 5′ M-MuLV LTR and a ΔMo+TTR(PD) 3′ LTR. This plasmid was then transfected into NIH 3T3 cells, and through the process of viral replication and subsequent infection of neighboring cells, resulting proviruses theoretically contained chimeric LTRs at both their 5′ and 3′ ends.

Transfected NIH 3T3 cultures showed evidence of infectious virus after three passages, as measured by the XC syncytial assay. From transfected and passaged XC$^+$ cultures, single-cell clones were isolated by plating at low density and selective trypsinization in cloning rings. Individual clones were scored for virus production by XC overlay, and their DNA was screened by Southern blot hybridization for the presence of integrated ΔMo+TTR(PD) M-MuLV provirus. It was important to confirm the presence of the ΔMo+TTR(PD) LTR in both 5′ and 3′ LTRs. To analyze 3′ LTRs, DNAs from individual clones were digested with *Sma*I and blots were probed with a ^{32}P-labeled DNA frag-

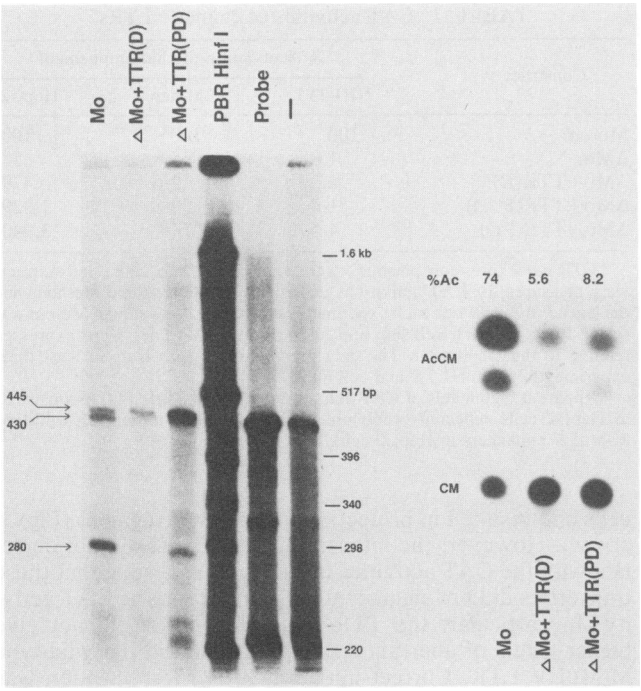

FIG. 3. Quantitative RNase T_2 protection analysis of transcripts in M-hep cells. Duplicate cultures of M-hep cells were transfected with the chimeric LTR-*cat* plasmids as shown. Total cytoplasmic RNA was prepared 48 h posttransfection from one culture for each plasmid, and 25 μg was hybridized with a uniformly labeled RNA probe spanning the LTR-*cat* gene junction (see Materials and Methods). The RNase T_2-resistant fragments were separated by electrophoresis in a 4.7% polyacrylamide gel containing 8 M urea. Correctly initiated *cat* gene transcripts (beginning at the M-MuLV cap site) were indicated by a 280-bp fragment. Aberrant transcripts initiating upstream of the *Xba*I site within the M-MuLV LTR were indicated by a 430-bp fragment. The pBR-*Hin*fI lane represents pBR322 DNA digested with *Hin*fI and end labeled with [α-^{32}P]ATP. The probe lane contained an antisense RNA probe not subjected to RNase digestion. Untransfected NIH 3T3 cytoplasmic RNA (minus lane) was subjected to the same analysis and showed nonspecific RNase protection of the original probe band (445 bp). The remaining cultures corresponding to the left three lanes of the left panel were harvested and assayed for CAT activity as described in the legend to Fig. 2 and are shown on the right. CM, Chloramphenicol; AcCM, acetylated form(s) of chloramphenicol; %Ac, percent acetylation.

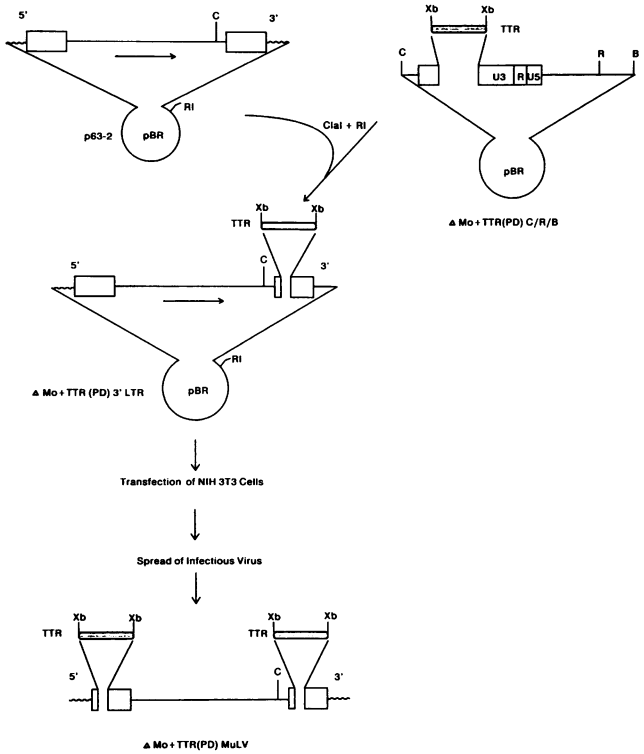

FIG. 4. Molecular cloning strategy for generation of ΔMo+TTR(PD) M-MuLV. Insertions of the TTR regulatory elements were first generated in ΔMoC/R/B, a plasmid subclone containing a single ΔMo LTR originally derived from a circularly permuted clone of M-MuLV DNA (described in reference 36). To generate infectious virus containing the chimeric LTR, the *Cla*I-to-*Eco*RI fragment of ΔMo+TTR(PD)C/R/B containing the altered LTR was cloned into the 3′ position of a molecular clone of integrated M-MuLV proviral DNA, p63-2. This yielded ΔMo+TTR(PD)3′LTR, a construct containing the wild-type M-MuLV LTR at the 5′ end and a chimeric LTR at the 3′ end. Transfection of this clone yielded proviruses with the chimeric LTRs at both the 5′ and 3′ ends [ΔMo+TTR(PD) M-MuLV] as a result of reverse transcription and viral spread (7).

ment corresponding to the *env* region (Fig. 5A). *Sma*I cleaves the M-MuLV LTR within the R region and readily distinguishes the wild-type 3′ LTR (2.05-kb fragment) from the ΔMo+TTR(PD) 3′ LTR (2.1-kb fragment) by size. ΔMo+TTR(PD) clones 6-4 (Fig. 5A, lane 3) and 6-6 (not shown) both showed the presence of the chimeric LTR at the 3′ end of the provirus. Clones showing a 2.05-kb fragment characteristic of the wild-type M-MuLV LTR (likely representing back recombinants with wild-type M-MuLV LTRs at both ends [36]) were excluded from further analysis (Fig. 5A, lane 2). Virus-producing single-cell clones isolated in this manner stably expressed virus without further rearrangement of the viral sequences.

Analysis of the 5′ LTRs in the cloned cell lines was facilitated by the presence of a unique *Pst*I site within the TTR promoter-proximal element (Fig. 1). Figure 5B shows Southern blot analysis of a *Pst*I restriction digest of several XC-positive clones hybridized with a probe encompassing the 5′ untranslated region of the M-MuLV provirus (*Sma*I to *Bst*EII). The ΔMo+TTR(PD) LTR in these clones was indicated by hybridization to a novel 720-bp fragment; most of the clones showed 5′ LTRs with the chimeric LTR.

The two transfected clones, 6-4 and 6-6 (Fig. 5B, lanes 5 and 7), were then used to prepare infectious virus stocks. Virus was harvested from these cultures, and the amount of infectious virus was quantified in a standard XC plaque assay. Typical titers of ΔMo+TTR(PD) were 4 orders of magnitude lower than those of wild-type M-MuLV stocks in the same assay (Table 2).

The relative infectivity of ΔMo+TTR(PD) M-MuLV on hepatocyte versus fibroblast lines was measured in endpoint dilution assays on M-hep and NIH 3T3 cells. This was done for technical reasons, since XC indicator cells would not form confluent monolayers in the presence of M-hep cells. Serial dilutions of wild-type and ΔMo+TTR(PD) M-MuLV stocks were used to infect M-hep and NIH 3T3 cells. After infection, cells were allowed to reach confluency and transferred for three cycles at a 1-to-5 ratio. The cell monolayers were UV irradiated, overlaid with XC cells, and scored for the presence or absence of syncytial plaques. The results are shown in Table 2. By this assay, the ΔMo+TTR(PD) M-MuLV stock had a dilution endpoint between 10^{-5} and 10^{-6} indicating a titer of 10^5 to 10^6 PFU/ml in NIH 3T3 cells.

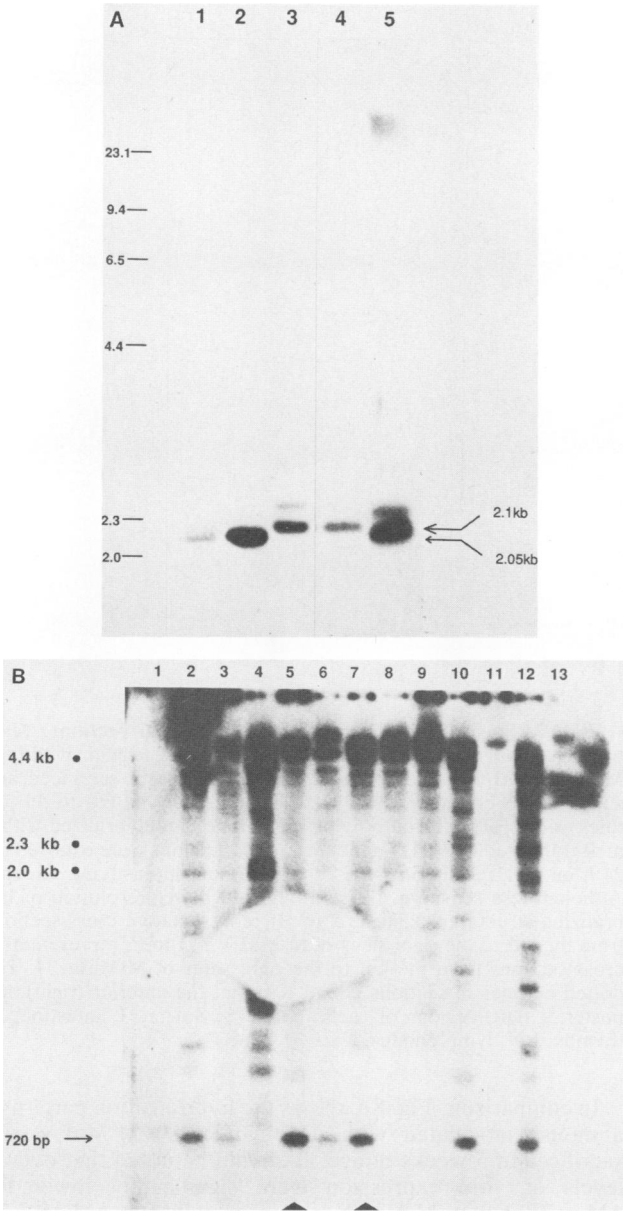

FIG. 5. Proviral DNAs of infected NIH 3T3 clones transfected with ΔMo+TTR(PD)3'LTR. (A) Southern analysis of the 3' LTR. Cloned cell lines transfected with ΔMo+TTR(PD)3'LTR were cultured until they showed uniform infection by the UV-XC overlay assay. High-molecular-weight DNA was extracted from XC$^+$ clones, digested with *Sma*I, and analyzed by Southern hybridization with an *env*-specific M-MuLV probe (the internal *Hpa*I fragment from 5.82 to 7.2 kb within the M-MuLV genome [17]). The presence of chimeric ΔMo+TTR(PD) in the 3' LTR was indicated by a 2.1-kb fragment (versus 2.05 kb for the wild-type M-MuLV LTR). Lanes: 1, clone 6-1; 2, clone 6-3; 3, clone 6-4; 4, ΔMo+TTR(PD)3'LTR plasmid DNA; 5, wild-type M-MuLV-infected NIH 3T3 DNA. Clones 6-4 and 6-6 (data not shown) both showed hybridization of a 2.1-kb fragment, and no hybridization was detected for the wild-type M-MuLV 2.05-kb fragment. These clones were subjected to further analysis (panel B). Hybridization of fragments larger than 2.1 kb in lanes 3 and 5 was due to incomplete digestion products, which is common in *Sma*I restriction digestions of M-MuLV proviral DNA (10). In this gel, the DNA in lane 5 migrated slowly because of an electrophoresis artifact; the major 2.05-kb fragment actually comigrated with the band in lane 2. (B) Southern blot analysis of the 5' LTR. High-molecular-weight DNA was digested with *Pst*I and analyzed by Southern blot hybridization with an M-MuLV 5'-specific probe (*Bst*II to *Sma*I; +28 to +725). Only cell clones containing the chimeric ΔMo+TTR(PD) LTR in the 5' LTR of the provirus showed hybridization of a 720-bp fragment. Lanes: 1, lambda *Hin*dIII-digested marker; 2, clone 6-1; 3, clone 6-2; 4, clone 6-3; 5, clone 6-4; 6, clone 6-5; 7, clone 6-6; 8, ΔMo+TTR(PD)3'LTR plasmid DNA mixed with uninfected NIH-3T3 DNA; 9, wild-type M-MuLV-infected NIH 3T3 cells; 10, clone 10-1; 11, clone 10-2; 12, clone 10-5; 13, clone 10-6. Clones used to prepare infectious viral stocks used for animal inoculation experiments are indicated by arrowheads in lanes 5 and 7. Note that the ΔMo+TTR(PD)3'LTR plasmid had a wild-type 5' LTR, so it would not give the 720-bp fragment. Hybridization in the high-molecular-weight region resulted from cross-hybridization to endogenous MuLV-related sequences. The DNAs in lanes 11 and 13 were underloaded, but at darker exposures, the 720-bp fragment was visible.

TABLE 2. Infectivity of chimeric M-MuLV

Assay and virus	Virus titer (PFU/ml)	
	NIH 3T3 cells	M-Hep cells
Standard XC syncytial assay[a]		
Wild-type M-MuLV	5.2×10^6	
ΔMo+TTR(PD) M-MuLV	5.3×10^2	
Endpoint dilution[b]		
Wild-type M-MuLV	10^7–10^8	10^6–10^7
ΔMo+TTR(PD) M-MuLV	10^5–10^6	10^4–10^5

[a] Tissue culture supernatants (24 h) were harvested from producer clones and clarified. Concentration of infectious virus was determined by infecting 10^6 NIH 3T3 cells, which had been pretreated for 1 h with 20 μg of Polybrene per ml, with various dilutions of supernatant. The cells were allowed to reach confluency and were scored for virus infection by the UV-XC overlay. Titers were calculated on the basis of numbers of syncytial plaques.

[b] After infection with serial 10-fold dilutions of the same supernatant stocks, cells were allowed to reach confluency and were then passaged at a 1-to-5 ratio. After three passages, NIH 3T3 cells were scored directly for virus infection by UV-XC overlay. Values were calculated on the basis of the highest dilution at which infected cultures were positive for virus after serial transfer. For example, for wild-type M-MuLV on NIH 3T3 cells, the cultures infected with the 10^{-7}-diluted stock gave XC plaques after transfer, whereas the 10^{-8} dilution did not.

This titer was higher by at least 3 orders of magnitude than that measured by the standard XC plaque assay. These differences between assays might result from relatively low RNA expression levels and viral spread of ΔMo+TTR(PD) M-MuLV virus in NIH 3T3 cells, which can affect the efficiency of XC plaque titration (18). Thus, titration by endpoint dilution assay more accurately reflected the actual titer of the viral stock. In contrast, titers of between 10^7 and 10^8 PFU/ml for wild-type M-MuLV were more similar to values determined by the XC plaque assay.

As another measure of the amount of virus in the stocks, RNAs were extracted from viral stocks and samples representing similar amounts of RNA were blotted onto a nylon membrane and used in an RNA dot blot assay (Fig. 6). Use of an M-MuLV *env* region hybridization probe showed that the ΔMo+TTR(PD) virus stocks had approximately 10- to 15-fold lower levels of viral RNA than did the M-MuLV virus stock, which correlated with the titers determined by the endpoint dilution assays of Table 2.

Endpoint dilution assays also indicated that wild-type M-MuLV had a slightly lower infectivity on M-hep hepatocytes than on NIH 3T3 fibroblasts (Table 2). In comparison, ΔMo+TTR(PD) M-MuLV also showed lower infectivity on

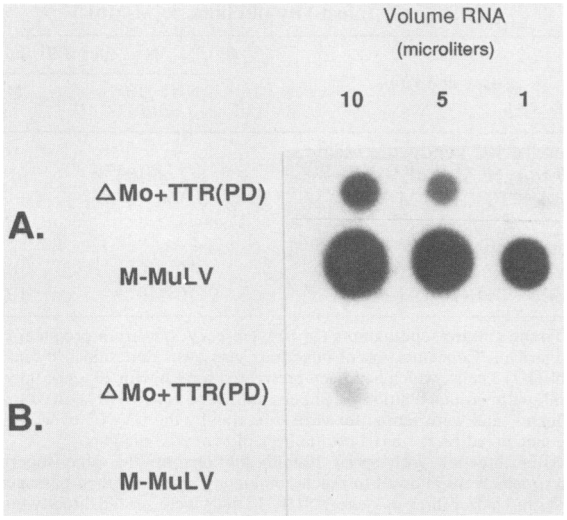

FIG. 6. Dot blot analysis of viral RNA. Viral stocks consisting of 24-h clarified tissue culture supernatants from 10^6 cells of either ΔMo+TTR(PD) M-MuLV clone 6-4 (viral stock A) or a wild-type M-MuLV-transfected NIH 3T3 culture were harvested by centrifugation (100,000 × *g*, 2 h). Viral RNA was extracted from the virus pellets, suspended, and dotted onto nylon membranes. Duplicate filters were made. Each microliter of viral RNA represented in the ΔMo+TTR(PD) M-MuLV lanes represents 0.7-fold as many cells as in the M-MuLV lanes. (A) Hybridization with an M-MuLV *env* probe. (B) Hybridization with a TTR probe (P and D sequence elements).

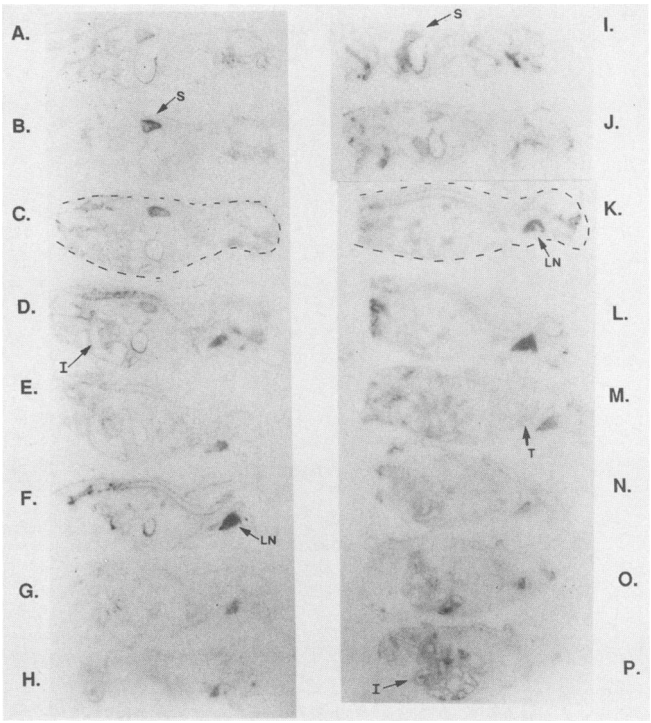

FIG. 7. In situ hybridization of whole animal sections. Mice were inoculated intraperitoneally at 2 days of age with wild-type M-MuLV. At 3.5 weeks of age, the animals were sacrificed and subjected to cryomicrotomy (32). Sagittal sections (20 to 40 μm thick) were cut, fixed onto nylon membrane, and hybridized with a nick-translated M-MuLV genomic probe. Sections were exposed for 24 h on high-resolution (XRP-5) film without intensifying screens. Although less sensitive, this film allowed better resolution of hybridizing structures. Panels: A to H, representative cross-sections from the left to the right sides of M-MuLV 3; I to P, representative cross-sections from the left to the right sides of M-MuLV 4. The dotted outlines in sections C and K orient the anterior (right) and posterior (left) regions of each animal. S, Spleen; I, intestine; T, thymus; LN, lymph nodes.

M-hep than on NIH 3T3 cells. Thus, both viruses had similar relative infectivities in hepatocytes and in fibroblasts in vitro; in particular, ΔMo+TTR(PD) M-MuLV did not have markedly higher infectivity on M-hep cells versus NIH 3T3 cells than did wild-type M-MuLV.

Inoculation of mice with ΔMo+TTR(PD) M-MuLV. It was also interesting to investigate in vivo replication of ΔMo+TTR(PD). Therefore, in situ hybridization of whole animal sections, as developed by Villareal (32), was used. Neonatal NFS/N mice were inoculated intraperitoneally with approximately 10^6 infectious units of wild-type M-MuLV or 10^4 infectious units (the highest titer available) of ΔMo+TTR(PD) M-MuLV per animal. At 3 to 5 weeks of age, animals were sacrificed, prepared for whole-mouse hybridization, and frozen in imbedding medium. Twelve representative cross-sections were taken across the sagittal plane of each animal and fixed onto nylon membranes. Sections were hybridized with a ^{32}P-labeled M-MuLV DNA probe under conditions favoring RNA-DNA hybridization. When this technique was used, patterns of hybridization to the membranes were indicative of viral transcription within specific regions of the animal (32, 40).

Figure 7 shows the hybridization pattern of two mice inoculated with wild-type M-MuLV and sacrificed at 3.5 weeks of age. Highest levels of wild-type M-MuLV expression generally occurred in the spleen and thymus, the target organs for M-MuLV replication. (Inoculation with our wild-type M-MuLV stocks resulted in negative or low hybridization patterns in the thymus in this particular litter of animals, but thymic hybridization was very strong for most other litters.) In addition, strong hybridization also occurred in cervical lymph nodes (also a known site for virus replication), as well as in the intestines.

In comparison, Fig. 8A shows the hybridization pattern of a mouse inoculated with ΔMo+TTR(PD) M-MuLV and sacrificed at 5 weeks of age. It should be noted that overall levels of viral expression were significantly lower for ΔMo+TTR(PD) M-MuLV than for wild-type M-MuLV, perhaps because of both the smaller inoculum and reduced infectivity of the chimeric virus. Mouse blots of ΔMo+TTR(PD) M-MuLV-inoculated animals required approximately fivefold longer exposure times to detect viral gene expression. As for wild-type M-MuLV, organs that showed high levels of viral expression for most of the animals analyzed were the thymus and spleen, indicating that substitution of the M-MuLV enhancers with the TTR regulatory sequences did not abrogate viral expression in these tissues. Hybridization also occurred in the intestines, indicating that ΔMo+TTR(PD) M-MuLV could replicate there as well. For comparison, uninfected mouse sections hybridized with the M-MuLV probe are shown in Fig. 8A, panels J and K.

Besides the sites of replication characteristic of wild-type M-MuLV, most of the animals inoculated with ΔMo+TTR(PD) M-MuLV (8 of 10) also showed hybridization to part of the brain. This pattern was unique to mice inoculated with ΔMo+TTR(PD) M-MuLV and did not appear in any of the animals inoculated in parallel with wild-type M-MuLV.

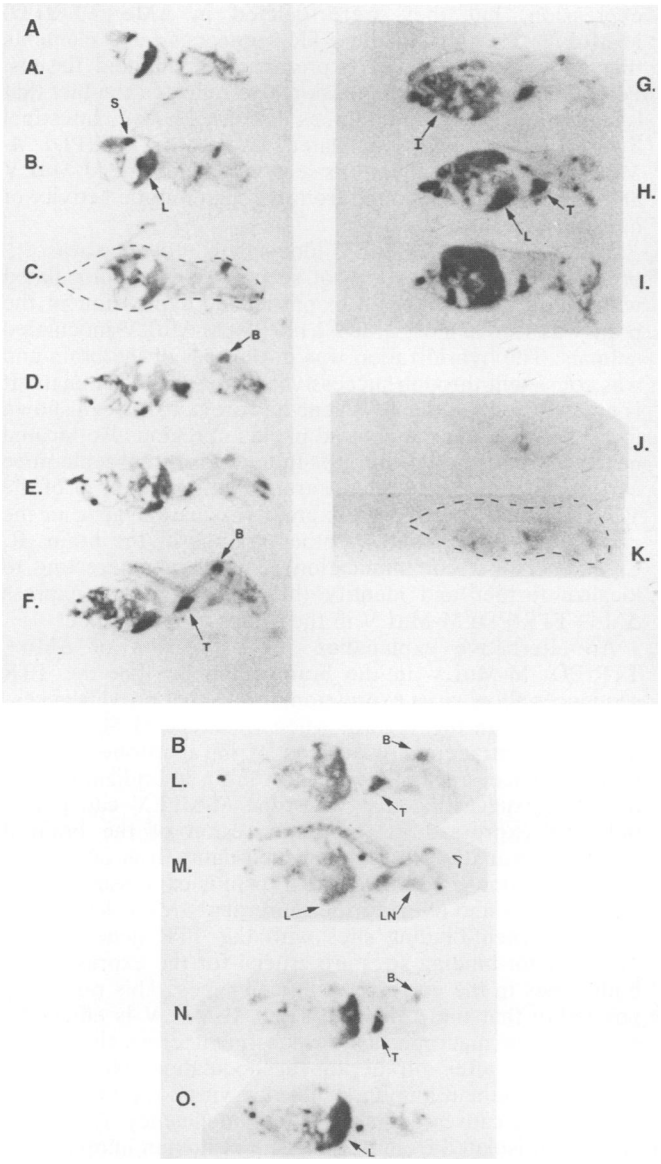

FIG. 8. In situ hybridization of whole sections of mice inoculated with ΔMo+TTR(PD) M-MuLV. Sections were hybridized with a nick-translated M-MuLV genomic probe and exposed for 5 days to Kodak high-sensitivity (XAR-5) film with intensifying screens. (A) A to I, Representative sections (left to right sides of the animal) of TTR9 (5 weeks old); J and K, sections of an uninoculated mouse hybridized with the same nick-translated M-MuLV genomic probe. The uninoculated sections correspond to panels B and G of TTR9, respectively, in approximate location within the animal. T, Thymus; S, spleen; I, intestine; LN, lymph nodes; B, brain; L, liver. (B) L and M, Representative sections of TTR3; N and O, representative sections of TTR4. These are successive sections in animals inoculated with ΔMo+TTR(PD) M-MuLV and correspond in approximate location to panels D and E and L and M of M-MuLV3 and M-MuLV4, respectively, in Fig. 7.

Wild-type M-MuLV-inoculated mice did show hybridization in the head, but this was associated with salivary or lymph glands near the mouth and, in some cases, with bone structures surrounding the brain. However, even at equivalent autoradiographic exposures, wild-type M-MuLV-inoculated animals did not show brain hybridization, while ΔMo+TTR(PD) M-MuLV-inoculated mice did.

TABLE 3. Tissue distribution of M-MuLV expression in whole animal sections analyzed by in situ hybridization

Litter and animal no.	Age (wks)	Viral stock[a]	Expression pattern[b]					
			T	S	B	L	I	LN
78								
TTR1	3	A	−	−	+	−	+	−
TTR2	3	A	+	−	+	−	+	−
89								
TTR3	3	A	+	+	+	+	+	+
TTR4	3	A	+	+	+	+	+	−
TTR8	5	A	+	+	+	−	+	Low
TTR9	5	A	+	+	+	+	+	−
97								
TTR5	4	A	+	+	+	−	+	−
TTR6	4	A	+	−	+	−	+	−
93; TTR7	3.5	B	+	+	−	−	+	−
97; TTR10	4.5	B	+	−	−	−	+	−
118								
M-MuLV1	3.5	C	+	+	−	−	+	+
M-MuLV2	3.5	C	+	+	−	−	+	+
M-MuLV3	3.5	C	−	+	−	−	+	+
M-MuLV4	3.5	C	Low	+	−	−	+	+

[a] Viral stock A represents ΔMo+TTR(PD) M-MuLV from clone 6-4; viral stock B is ΔMo+TTR(PD) M-MuLV from clone 6-6; viral stock C is wild-type M-MuLV (clone 43D).

[b] T, Thymus; S, spleen; B, brain; L, liver; I, intestine; LN, cervical lymph node.

Additionally, among animals inoculated with ΔMo+TTR(PD) M-MuLV from one particular litter (no. 89), three of four animals analyzed showed viral expression in the liver (Fig. 8; Table 3). None of the mice inoculated with M-MuLV showed this hybridization pattern. Hybridization patterns of two additional animals inoculated with ΔMo+TTR(PD) M-MuLV, TTR3 and TTR4, are shown in Fig. 8B, panels L to O. These results suggest that the ΔMo+TTR(PD) LTR conferred expanded tissue tropism to M-MuLV, allowing replication in the brain and (in some cases) liver. A summary of the hybridization patterns seen in whole-mouse hybridization studies is shown in Table 3.

To ensure that organs within the mice showing hybridization contained the ΔMo+TTR(PD) M-MuLV provirus, frozen tissue was recovered from the target organs of some animals during serial sectioning and DNA was extracted. By using TTR sequence elements as probes on Southern blots of DNA, ΔMo+TTR(PD) M-MuLV provirus was detected in a number of tissues, including the brain of animal TTR5 (data not shown). In instances in which detection of ΔMo+TTR(PD) M-MuLV by direct Southern blot analysis was difficult, amplification by polymerase chain reaction confirmed the presence of the chimeric provirus in tissues from several animals. While these experiments confirmed the presence of virus related to the inoculated ΔMo+TTR(PD) M-MuLV, it was also possible that alterations occurred in vivo (see below).

DISCUSSION

These experiments studied chimeric M-MuLV LTRs containing cellular regulatory sequences from the mouse TTR gene. Insertions of the TTR distal enhancer, alone or in conjunction with the promoter-proximal element, yielded

M-MuLV LTRs with increased activity in hepatocyte cell lines relative to NIH 3T3 fibroblasts. Our results supported previous findings that the TTR promoter-proximal and distal enhancer sequences can confer differential expression of a marker gene in liver-derived cell types. The TTR–M-MuLV chimeric LTRs were also expressed in HepG2 cells, a human cell line normally nonpermissive for expression from the wild-type M-MuLV LTR. Constructs containing both TTR promoter-proximal and distal enhancer sequences [ΔMo+TTR(PD) and ΔMo+TTR(P⁻D)] showed higher levels of CAT activity than did constructs containing only the distal enhancer [ΔMo+TTR(D)]. This suggests that the TTR promoter-proximal element augmented expression synergistically with the TTR distal enhancer, even when inserted upstream. Furthermore, the cooperative effect was independent of the orientation of the promoter-proximal element, suggesting that the promoter-proximal element also contains tissue-specific enhancer sequences. This is consistent with the ability of the promoter-proximal sequences to support low levels of tissue-specific expression of a marker gene, even in the absence of the TTR distal enhancer (5).

ΔMo+TTR(PD) M-MuLV is the first replication-competent M-MuLV whose LTR is driven by cellular regulatory sequences. In tissue culture, in comparison with wild-type M-MuLV, ΔMo+TTR(PD) M-MuLV had similar infectivity in NIH 3T3 cells and hepatocytes. It should be noted that the assay used would have measured only relatively large differences (greater than 10-fold) between the infectivities of these viruses.

Although the relative infectivity for hepatocytes shown by ΔMo+TTR(PD) M-MuLV in vitro was similar to that of wild-type M-MuLV, this chimeric virus showed an expanded range of expression when inoculated into mice. In situ hybridization of whole animal sections was a convenient and rapid method of mapping viral expression within an inoculated animal. In previous experiments using analyses of isolated organs, wild-type M-MuLV-inoculated animals showed evidence of viral infection in most lymphoid organs, including the thymus (the target of disease [45]), well before onset of the end-stage tumor (23). By in situ hybridization, mice inoculated intraperitoneally with wild-type M-MuLV showed high levels of M-MuLV expression in lymphoid tissues, such as spleen, thymus, and cervical lymph nodes, in agreement with earlier experiments.

Hybridization in the intestines of mice inoculated with wild-type M-MuLV was unexpected, since previous studies indicated that neonatal inoculation of M-MuLV resulted in detectable virus expression only in hematopoietic organs (24). Productive retrovirus infection has previously been shown to be most efficient in actively dividing cells (23, 37). Intestinal epithelial cells are a rapidly dividing cell type and might therefore support high levels of M-MuLV replication. This hybridization pattern also occurred in mice inoculated intracranially with wild-type M-MuLV, indicating that it did not simply reflect efficient virus expression near the site of intraperitoneal inoculation. More refined analysis, such as immunocytochemistry, might further elucidate the intestinal cell type(s) involved. In Mov-1 mice, which activate a genetically transmitted M-MuLV shortly after birth, virus infection in the intestines was localized to gut-associated lymphoid cells by immunocytochemistry (23, 24).

Like wild-type M-MuLV, animals inoculated intraperitoneally with ΔMo+TTR(PD) M-MuLV also showed high levels of virus expression in the spleen and thymus. This was surprising, since the M-MuLV enhancers have previously been implicated as important determinants in lymphoid expression, but they were deleted in ΔMo+TTR(PD) M-MuLV. Presumably the TTR sequences have elements that allow at least some expression in lymphoid tissues. Perhaps the lymphoid expression also reflected the fact that lymphoid cells divide rapidly, as discussed above. Intestinal hybridization in mice inoculated with ΔMo+TTR(PD) M-MuLV resembled the patterns seen with wild-type M-MuLV and may also have resulted from the high mitotic activity of intestinal cells.

ΔMo+TTR(PD) M-MuLV inoculated into mice was expressed in two novel sites not seen for animals inoculated with wild-type M-MuLV. In particular, expression in the brain was seen in most ΔMo+TTR(PD) M-MuLV-inoculated animals. The hybridization was in the rear of the brain and was consistent through successive sections in the animals. It is noteworthy that the TTR gene has previously been shown to be expressed in the choroid plexus, a region also located near the back of the brain (9). In addition, transgenic mice carrying a marker gene under transcriptional control of the TTR regulatory sequences express the marker gene in the choroid plexus, as well as other regions of the brain (R. Costa, personal communication). It will be interesting to localize further and identify the cell types that express ΔMo+TTR(PD) M-MuLV in the brains of these mice.

An alternative explanation for expression of ΔMo+TTR(PD) M-MuLV in the brain could be that the TTR sequences allow virus expression in cells that provide access to the brain. In this regard, when wild-type M-MuLV was inoculated intracranially (instead of intraperitoneally) into newborn mice, a similar pattern of brain hybridization was observed, suggesting that wild-type M-MuLV can potentially be expressed in the same region of the brain if delivered near this site (unpublished data). It is interesting that the murine gene for α1 antitrypsin is expressed in both macrophages and liver; furthermore, it shares at least three nuclear protein-binding sites with the TTR gene (4, 16). These factor-binding sites are crucial for the expression of both genes in the corresponding cell types. This raises the possibility that the ΔMo+TTR(PD) M-MuLV is efficiently expressed in macrophages, which might cross the blood-brain barrier after intraperitoneal inoculation. Neurotropic variants of human immunodeficiency virus, the human retrovirus that causes acquired immunodeficiency syndrome, have been isolated from brain tissue of human immunodeficiency virus-infected individuals; these isolates also infect macrophages and monocytes more efficiently than do human immunodeficiency virus isolates from other tissues (27).

Initially it seemed that the most likely site for ΔMo+TTR(PD) M-MuLV expression in vivo might be the liver. Indeed, 3 of 10 animals inoculated with ΔMo+TTR(PD) M-MuLV showed viral expression in the liver, supporting the notion that the TTR regulatory elements conferred liver-specific expression to the virus. In situ hybridization of sections from mice inoculated with wild-type M-MuLV (as well as M-MuLVs with other chimeric LTRs) have never shown detectable hybridization to the liver. It was noteworthy that all three animals showing hybridization to the liver came from the same litter. Since all inoculations were into inbred NFS/N mice, host genetic factors were not responsible for the high expression in that particular litter. Perhaps a secondary factor, such as another infectious agent, in that litter may have played a role in allowing virus expression in the liver. Identification of such a secondary factor might provide further insight into obtaining retroviral gene expression in cells of this organ.

The mammalian liver is an important target organ for gene

transfer (51). Previous studies using M-MuLV vectors have shown that newborn, as well as adult, liver cells are refractile to retrovirus infection in vivo. Our results suggest that under certain conditions, infection of neonatal NFS/N mice with ΔMo+TTR(PD) M-MuLV can lead to persistent viral gene expression in the liver, detectable for up to 5 weeks after birth. The ΔMo+TTR(PD) M-MuLV chimeric provirus might provide a useful model system for studying retroviral expression in this organ.

It should be noted that while M-MuLV driven by the ΔMo+TTR(PD) LTR had expanded sites of replication in the animal in comparison with wild-type M-MuLV, these experiments did not exclude the possibility that alterations in the LTR took place during passage in vivo. It is possible that additional mutations or rearrangements in the enhancers (or other regions) occurred, allowing virus replication in different tissues. Southern blot and polymerase chain reaction experiments established the presence of TTR sequences in the infected tissues, but they did not rule out subtle changes. Nevertheless, animals inoculated with ΔMo+TTR(PD) M-MuLV showed novel sites of replication in comparison with wild-type M-MuLV. Thus, regardless of whether secondary mutations contributed, the TTR enhancers conferred an expanded range of tissue infection.

In situ hybridization of whole mouse sections is a valuable tool for identifying novel sites of viral replication within an animal (32). While this technique allows rapid identification of interesting tissues, it also has limitations. In particular, this technique does not readily lend itself to analysis of the same samples at the microscopic level. Thus, for complicated organs, such as the brain, association of hybridization with specific structures is difficult. Likewise, identification of which cells within an organ are virus infected is not feasible. To answer such questions, more refined techniques, such as immunohistochemistry or in situ hybridization at the microscopic level, will be necessary. Future experiments with ΔMo+TTR(PD) M-MuLV will use these techniques.

Mice inoculated with ΔMo+TTR(PD) M-MuLV have shown a low level of disease so far, even though the virus is expressed in the same target tissues as is wild-type M-MuLV. We have previously described increased latency of disease in mice inoculated with an altered M-MuLV with a ΔMo LTR containing simian virus 40 enhancers (18). The lower rate of in vivo expression and replication of ΔMo+TTR(PD) M-MuLV may also contribute to the extended latency of disease. Further studies will determine whether infection with ΔMo+TTR(PD) M-MuLV ultimately results in tumors and, furthermore, whether the disease type is similar to or different from wild-type M-MuLV-induced leukemia.

ACKNOWLEDGMENTS

This work was supported by Public Health Service grants CA32454 and CA32455 from the National Institutes of Health to H.F. G.F. was supported by Public Health Service training grant T32 GM07134 from the National Institutes of Health during some of this work. Support of the Cancer Research Institute, University of California, Irvine, is acknowledged.

We are indebted to Robert Costa for providing *TTR* sequence element clones and many valuable comments and discussions. We thank Dieter Paul for providing M-hep cells. We also thank Luis Villarreal and Rosemary Rochford-Sun for advice on the in situ hybridization protocol.

LITERATURE CITED

1. **Brightman, B. K., P. K. Pattengale, and H. Fan.** 1986. Generation and characterization of a recombinant Moloney murine leukemia virus containing the v-*myc* oncogene of avian MC29 virus: in vitro transformation and in vivo pathogenesis. J. Virol. **60**:68–81.
2. **Campos, R., and L. P. Villarreal.** 1982. An SV-40 deletion mutant accumulates late transcripts in a paranuclear extract. Virology **119**:1–11.
3. **Chen, C., and H. Okayama.** 1987. High-efficiency transformation of mammalian cells by plasmid DNA. Mol. Cell. Biol. **7**:2745–2752.
4. **Costa, R. H., D. R. Grayson, and J. E. Darnell, Jr.** 1989. Multiple hepatocyte-enriched nuclear factors function in the regulation of transthyretin and α1-antitrypsin genes. Mol. Cell. Biol. **9**:1415–1425.
5. **Costa, R. H., E. Lai, and J. E. Darnell, Jr.** 1986. Transcriptional control of the mouse prealbumin (transthyretin) gene: both promoter sequences and a distinct enhancer are cell specific. Mol. Cell. Biol. **6**:4697–4708.
6. **Costa, R. H., E. Lai, D. R. Grayson, and J. E. Darnell, Jr.** 1988. The cell-specific enhancer of the mouse transthyretin (prealbumin) gene binds a common factor at one site and a liver-specific factor(s) at two other sites. Mol. Cell. Biol. **8**:81–90.
7. **Davis, B., E. Linney, and H. Fan.** 1985. Suppression of leukaemia virus pathogenicity by polyoma virus enhancers. Nature (London) **314**:550–553.
8. **des Groseillers, L., and P. Jolicoeur.** 1984. The tandem repeats within the long terminal repeat of murine leukemia viruses are the primary determinant of their leukemogenic potential. J. Virol. **52**:945–952.
9. **Dickson, P. W., G. S. Howlett, and G. Schreiber.** 1985. Rat transthyretin (prealbumin) molecular cloning nucleotide sequence and gene expression in liver and brain. J. Biol. Chem. **260**:8214–8219.
10. **Fan, H., H. Chute, E. Chao, and P. K. Pattengale.** 1988. Leukemogenicity of Moloney murine leukemia virus carrying polyoma enhancer sequences in the long terminal repeat is dependent on the nature of the inserted polyoma sequences. Virology **166**:58–65.
11. **Fan, H., S. Mittal, H. Chute, E. Chao, and P. K. Pattengale.** 1986. Rearrangements and insertions in the Moloney murine leukemia virus long terminal repeat alter biological properties in vivo and in vitro. J. Virol. **60**:204–214.
12. **Feinberg, A. P., and B. Vogelstein.** 1983. A technique for radiolabeling DNA restriction endonuclease fragments to high specific activity. Anal. Biochem. **132**:6–13.
13. **Feuer, G., M. Taketo, R. C. Hanecak, and H. Fan.** 1989. Two blocks in Moloney murine leukemia virus expression in undifferentiated F9 embryonal carcinoma cells as determined by transient expression assays. J. Virol. **63**:2317–2324.
14. **Golemis, E., Y. Li, T. N. Frederickson, J. W. Hartley, and N. Hopkins.** 1989. Distinct segments within the enhancer region collaborate to specify the types of leukemia induced by nondefective Friend and Moloney viruses. J. Virol. **63**:328–337.
15. **Gorman, C. M., L. F. Moffat, and B. H. Howard.** 1982. Recombinant genomes which express chloramphenicol acetyltransferase in mammalian cells. Mol. Cell. Biol. **2**:1044–1051.
16. **Grayson, D. R., R. H. Costa, K. G. Xanthopoulos, and J. E. Darnell, Jr.** 1988. A cell-specific enhancer of the mouse α1-antitrypsin gene has multiple functional regions and corresponding protein-binding sites. Mol. Cell. Biol. **8**:1055–1066.
17. **Hanecak, R., S. Mittal, B. R. Davis, and H. Fan.** 1986. Generation of infectious Moloney murine leukemia viruses with deletions in the U3 portion of the long terminal repeat. Mol. Cell. Biol. **6**:4634–4640.
18. **Hanecak, R., P. K. Pattengale, and H. Fan.** 1988. Addition or substitution of simian virus 40 enhancer sequences into the Moloney murine leukemia virus (M-MuLV) long terminal repeat yields infectious M-MuLV with altered biological properties. J. Virol. **62**:2427–2436.
19. **Herbomel, P., P. Bourachot, and M. Yaniv.** 1984. Two distinct enhancers with different cell specificities coexist in the regula-

tory region of polyoma. Cell **39**:653–662.
20. **Hoffmann, B., A. Piasecki, and D. Paul.** 1989. Proliferation of fetal rat hepatocytes in response to growth factors and hormones in primary culture. J. Cell. Physiol. **139**:654–662.
21. **Hollon, T., and F. K. Yoshimura.** 1989. Mapping of functional regions of murine retrovirus long terminal repeat enhancers: enhancer domains interact and are not independent in their contributions to enhancer activity. J. Virol. **63**:3353–3361.
22. **Ishimoto, A., M. Takimoto, A. Adachi, M. Kakuyama, S. Kato, K. Kakimi, F. Fukuoka, T. Ogiu, and M. Matsuyama.** 1987. Sequences responsible for erythroid and lymphoid leukemia in the long terminal repeats of Friend-mink cell focus-forming and Moloney leukemia viruses. J. Virol. **61**:1861–1866.
23. **Jaenisch, R.** 1979. Moloney leukemia virus gene expression and gene amplification in preleukemic and leukemic BALB/Mo mice. Virology **93**:80–90.
24. **Jaenisch, R.** 1980. Retroviruses and embryogenesis: microinjection of Moloney murine leukemia virus into midgestation mouse embryos. Cell **19**:181–188.
25. **Kitado, H., I. S. Y. Chen, N. P. Shah, A. J. Cann, K. Shimotohno, and H. Fan.** 1987. U3 sequences from HTLV I and II LTRs confer pX protein response to a murine leukemia virus LTR. Science **235**:901–904.
26. **Knowles, B., C. C. Howe, and D. P. Anden.** 1980. Human hepatocellular carcinoma cell lines secrete the major plasma proteins and hepatitis B surface antigen. Science **290**:497–499.
27. **Koyanagi, Y., S. Miles, R. T. Mitsuyasu, J. E. Merrill, H. V. Vinters, and I. S. Y. Chen.** 1987. Dual infection of the central nervous system by AIDS viruses with distinct cellular tropism. Science **236**:819–822.
28. **Laimins, L. A., P. Gruss, R. Pozzatti, and G. Khoury.** 1984. Characterization of enhancer elements in the long terminal repeat of Moloney murine sarcoma virus. J. Virol. **49**:183–189.
29. **Lenz, J. D., D. Celander, R. L. Crowther, R. Patarca, D. W. Perkins, and W. A. Haseltine.** 1984. Determination of the leukemogenicity of a murine retrovirus by sequences within the long terminal repeat. Nature (London) **308**:467–470.
30. **Li, Y., E. Golemis, J. W. Hartley, and N. Hopkins.** 1987. Disease specificity of nondefective Friend and Moloney murine leukemia viruses is controlled by a small number of nucleotides. J. Virol. **61**:693–700.
31. **Linney, E., B. Davis, J. Overhauser, E. Chao, and H. Fan.** 1984. Non-function of Moloney murine leukemia virus regulatory sequence in F9 embryonal carcinoma cells. Nature (London) **308**:470–472.
32. **Lipkin, W. I., L. P. Villarreal, and M. B. A. Oldstone.** 1989. Whole animal section *in situ* hybridization and protein blotting: new tools in molecular analysis of animal models for human disease. Curr. Top. Microbiol. Immunol. **143**:33–87.
33. **Maniatis, T., E. F. Fritsch, and J. Sambrook.** 1982. Molecular cloning: a laboratory manual. Cold Spring Harbor Laboratory, Cold Spring Harbor, N.Y.
34. **Manley, N. R., M. A. O'Connell, P. A. Sharp, and N. Hopkins.** 1989. Nuclear factors that bind to the enhancer region of nondefective Friend murine leukemia virus. J. Virol. **63**:4210–4223.
35. **Melton, D. A., P. A. Krieg, M. R. Rebagliati, T. Maniatis, K. Zinn, and M. R. Green.** 1984. Efficient *in vitro* synthesis of biologically active RNA and RNA hybridization probes from plasmids containing a bacteriophage SP6 promoter. Nucleic Acids Res. **12**:7035–7056.
36. **Overhauser, J., and H. Fan.** 1985. Generation of glucocorticoid-responsive Moloney murine leukemia virus by insertion of regulatory sequences from murine mammary tumor virus in the long terminal repeat. J. Virol. **54**:133–144.
37. **Paskind, M. D., R. A. Weinberg, and D. Baltimore.** 1975. Dependence of Moloney murine leukemia virus production on cell growth. Virology **67**:242–248.
38. **Paul, D., M. Hohne, C. Pinkert, A. Piasecki, E. Ummelmann, and R. L. Brinster.** 1988. Immortalized differentiated hepatocyte lines derived from transgenic mice harboring SV40 T-antigen genes. Exp. Cell Res. **175**:354–362.
39. **Rigby, P. W. J., M. Dieckman, C. Rhodes, and P. Berg.** 1977. Labeling deoxyribonucleic acid to high specific activity in vitro by nick translation with DNA polymerase I. J. Mol. Biol. **113**:231–251.
40. **Rochford, R., B. A. Campbell, and L. P. Villarreal.** 1987. A pancrease specificity results from the combination of polyoma virus and Moloney murine leukemia virus enhancer. Proc. Natl. Acad. Sci. USA **84**:449–453.
41. **Rowe, W. P., W. E. Pugh, and J. W. Hartley.** 1970. Plaque assay technique for murine leukemia viruses. Virology **42**:1136–1139.
42. **Sen, R., and D. Baltimore.** 1986. Multiple nuclear factors interact with the immunoglobulin enhancer sequences. Cell **46**:705–711.
43. **Staudt, L. M., H. Singh, R. Sen, T. Wirth, P. A. Sharp, and D. Baltimore.** 1986. A lymphoid-specific protein binding to the octamer motif of immunoglobulin genes. Nature (London) **323**: 640–643.
44. **Swift, G. H., R. E. Hammer, R. J. MacDonald, and R. L. Brinster.** 1984. Tissue-specific expression of the rat pancreatic elastase I gene in transgenic mice. Cell **38**:639–649.
45. **Teich, N., J. Wyke, T. Mak, A. Bernstein, and W. Hardy.** 1982. Pathogenesis of retrovirus-induced disease, p. 785–998. *In* R. Weiss, N. Teich, J. Coffin, and H. E. Varmus (ed.), RNA tumor viruses. Cold Spring Harbor Laboratory, Cold Spring Harbor, N.Y.
46. **Theisen, M., A. Stief, and A. E. Sippel.** 1986. The lysozyme enhancer: cell-specific activation of the chicken lysozyme gene by a far upstream DNA element. EMBO J. **5**:719–729.
47. **Todaro, G. J., and H. Green.** 1963. Quantitative studies of the growth of mouse embryo cells in culture and their development into established lines. J. Cell Biol. **17**:299–313.
48. **Varmus, H. E., and R. S. Swanstrom.** 1982. Replication of retroviruses, p. 369–512. *In* R. Weiss, N. Teich, J. Coffin, and H. E. Varmus (ed.), RNA tumor viruses. Cold Spring Harbor Laboratory, Cold Spring Harbor, N.Y.
49. **Walker, M. D., T. Edlund, A. M. Boulet, and W. J. Rutter.** 1983. Cell-specific expression controlled by the 5′-flanking region of insulin and chymotrypsin genes. Nature (London) **306**:557–561.
50. **Wasylyk, B. C., C. Wasylyk, P. Augereau, and P. Chambon.** 1983. The SV-40 72 bp repeat preferentially potentiates transcription starting from proximal natural or substitute promoter elements. Cell **32**:503–514.
51. **Wolff, J. A., J. K. Yee, H. F. Skelly, J. C. Moores, J. G. Respess, T. Friedman, and H. Leffert.** 1987. Expression of retrovirally transduced genes in primary cultures of adult rat hepatocytes. Proc. Natl. Acad. Sci. USA **84**:3344–3348.
52. **Wu, L., B. J. Morley, and R. D. Campbell.** 1987. Cell-specific expression of the human complement protein factor B gene: evidence for the role of two distinct 5′-flanking elements. Cell **48**:331–342.